A macro model of silicon spiral inductor

C.Y. Su [a,*], L.P. Chen [b], S.J. Chang [a], B.M. Tseng [b], D.C. Lin [b], G.W. Huang [b],
Y.P. Ho [b], H.Y. Lee [b], J.F. Kuan [b], W.Y. Wen [c], P. Liou [c], C.L. Chen [c],
L.Y. Leu [c], K.A. Wen [d], C.Y. Chang [d]

[a] *Department of Electrical Engineering, National Cheng Kung University, 1 University Road, Tainan, Taiwan, ROC*
[b] *National Nano Device Laboratories, 1001-1 Ta Hsueh Road, Hsinchu, Taiwan, ROC*
[c] *Winbond Electronics Corporation, Li Hsin Road, Science Based Industrial Park, Hsinchu, Taiwan, ROC*
[d] *Department of Electronics Engineering and Institute of Electronics, National Chiao Tung University, Hsinchu, Taiwan, ROC*

Abstract

A new automatic parameter extraction method for modeling of silicon spiral inductors is presented. The concepts on self-resonance frequency (f_{sr}) and quality factor of a spiral inductor are utilized to develop the concise extraction procedures. In the mean time, the presented extraction procedures are programmed as a macro to execute all the extractions automatically and shorten the extraction time effectively. Without any additional optimization or curve fitting, almost all the patterns of *S*-parameters between the measured and the simulation of extracted data implemented with the extraction macro are less than 5%. The programmed extraction macro makes it fast and accurate to extract and characterize the behaviors of silicon-based spiral inductors with different structures and substrate resistivities. It provides a concrete foundation for commercial silicon radiofrequency (RF) circuit design to realizing on-chip silicon RF integrated circuits. Furthermore, the directly extracted equivalent model parameters, without any optimization, also provide a rule to fairly, effectively and physically judge the performance of a spiral inductor. © 2002 Elsevier Science Ltd. All rights reserved.

Keywords: Spiral inductor; Radiofrequency (RF); Programmed extraction macro

1. Introduction

With the dramatic advancement of Si VLSI technologies, the system-on-chip (SOC) silicon radiofrequency (RF) integrated circuit has recently emerged as an attractive candidate to satisfy the rapidly growing wireless communication applications [1–5]. The wireless communication applications based on Si technologies can increase the integration density of RF module, baseband and digital signal processing (DSP) modules, etc. Therefore, both the reliability and production cost of Si-based RF integrated circuits (RFICs) can be improved as compared to those of compound RF circuits. There are many widely used frequency range of personal wireless communication applications just lying in low GHz, such as 0.9 GHz of global system for mobile communication (GSM) system, 1.8 GHz of digital communication system (DCS) system and 2.4 GHz of Bluetooth technology. As a result, the performance of Si RF components in the frequency range of low GHz is a very important issue for realizing on-chip Si RFICs.

Unfortunately, semi-conducting silicon substrate produces substrate loss effect and dramatically degrades the performance of Si components at microwave frequency range [6–12]. Among the Si-based RF components, silicon spiral inductor plays one of important roles. The inductors can be used in many applications of RF circuits, such as impedance matching of low-noise amplifier, on-chip filtering, etc. [1–6]. However, the loss effect of Si substrate makes the performance of inductors

---

Nomenclature

f_{sr}	self-resonance frequency, Hz	R_{sub1} and R_{sub2}	equivalent substrate parasitic resistance, Ω
ω_{sr}	self-resonance angular frequency, rad/s		
R_s	series resistance of the inductor, Ω	C_{sub1} and C_{sub2}	equivalent substrate parasitic capacitance, fF
L_s	series inductance of the inductor, nH		
C_p	fringing capacitance of the adjacent metal traces, fF	δ	the deviation between the ideal and real quality factor
C_{ox1} and C_{ox2}	the capacitance between spiral metal layers and substrate, fF	π	the pi constant
		f	the operation frequency, Hz

---

change tremendously with various operation frequencies. As a result, accurate and convenient equivalent circuit model of silicon inductor, that describes the behavior of inductor at certain frequency, plays a very important role for on-chip silicon RF integrated circuit designs.

To achieve the goal of extracting the equivalent model parameters of silicon inductors and model the inductors' characteristics accurately for RF circuit design, a convenient and fast extraction method, only from the measured *S*-parameters without any additional test structures, is presented in this paper. Besides, the presented extraction procedures are programmed as a powerful macro according to the extraction algorithms to execute all the extraction procedures automatically and shorten the extraction time effectively. In the mean time, the spiral inductors with different structures and different substrate resistivities have also been analyzed to verify the accuracy and convenience of the extraction macro. Furthermore, the extracted equivalent parameters of inductors can be adopted as the initial values of optimization or curve fitting, if necessary, to obtain the user-desired inductor model parameters for RF circuit simulation.

2. Extraction methods of silicon inductor model

The most important issue on designing silicon spiral inductors is to obtain inductors with desired inductance values and high enough quality factors at the same time. To achieve it, the structure and layout geometry of the inductors must be designed well to induce the magnetic coupling between spiral windings, to reduce the series resistance of the inductors' metal spirals and improve the loss effect from substrate. Increasing the metal thickness [9,10], shunting multi-level metals [8,12] or using the metal with lower resistivity [11] all help to reduce the metal series resistance of the inductors. Thicker dielectric layer below the metal spiral [10,13] or utilizing substrates with higher resistivities [9–11,14] both can reduce the loss effect of Si substrate. Besides, the center

of the inductors should have considerable space to allow the passing of the magnetic flux [10]. The spacing between adjacent metal lines should be downsized adequately to optimize the magnetic coupling. The introduction of the patterned ground shielding [15] or removing the silicon underneath spiral inductor [5] also improves the loss effect of silicon substrate. The design of silicon spiral inductors is really a state of the art and involves a complex trade-off between the various layout geometry and process parameters.

In the reported literature, the most popular extraction methods of equivalent inductor parameters are utilizing the electromagnetic (EM) simulation [8,10,16,17] or fitting the simulated results to the measured data by circuit simulator or parameter optimization tool [9,14,18,19]. The popular EM simulation tools include momentum and high frequency structure simulator (HFSS) of Agilent-EEsof, etc. Although the EM simulation theoretically can provide the simulation results with considerable accuracy, however, the processing time of EM simulation generally takes several hours or even longer time. Besides, the extracted results by EM simulation often cannot provide sufficient physical meanings, and sometimes even the EM simulation cannot converge to produce reasonable results successfully.

Another kind of widely used methods that utilize curve fitting or parameter optimization by circuit simulator or optimization tool, such as the advanced design system (ADS) circuit simulator or LIBRA of Agilent-EEsof, always require fine-tuning of parameters repeatedly. The procedure of repeated fine-tuning or optimization generally cannot be finished very soon. In the mean time, the finally extracted parameters from parameter tuning or optimization are not unique for the same inductor. That is, we can obtain many sets of inductor parameters that all seem to model the behavior of the same inductor well, even though the extracted parameters are not reasonable. The nonuniqueness of the extracted results implies that the method by curve fitting makes the extracted results own less physical meanings. The methods by curve fitting or parameter optimization

Table 1
The programmed extraction macro reflecting the dependence of the equivalent circuit parameters on different inductor structures physically

Device	Sub-resistance (Ωcm)	ILD (μm)	Metal 1 (μm)	IMD 1 (μm)	Metal 2 (μm)	IMD 2 (μm)	Metal 3 (μm)	Q_{max}	Frequency @ Q_{max} (GHz)	R_s (Ω)	L_s (nH)	C_P (fF)	C_{ox1} (fF)	C_{ox2} (fF)	R_{sub1} (Ω)	R_{sub2} (Ω)	C_{sub1} (fF)	C_{sub2} (fF)
W13	15–25	0.9	0.45	0.85	0.45	0.85	1	5.9	3.1	6.30	4.3	20.4	935.6	755.9	840.9	694.8	12.9	20.1
W8	1.6–2.4k			0.85	0.45	0.85	1	9.2	4.9	5.78	4.09	23.7	369.7	417.0	1.810k	1.425k	13.7	21.1
W21	15–25			1.5	0.8	1.5	2	7.3	2.5	3.75	4.01	19.8	755.0	751.3	678.9	575.3	13.6	22.3
W24	1.6–2.4k			1.5	0.8	1.5	2	11.6	5.0	4.40	4.03	20.0	127.8	169.1	2.271k	1.849k	13.3	20.6
W15	15–25	The same with W13 but with an additional 0.8 μm trench oxide below ILD.						6.2	3.1	6.22	4.52	19.3	519.8	676.5	894.9	738.3	13.1	20.6

lower the capability of providing systematic rules to characterize the performance of silicon spiral inductors fairly, effectively and physically.

In order to overcome the disadvantage of the EM simulation and curve fitting methods, a programmed extraction macro based on the proposed extraction algorithms is presented to extract equivalent circuit parameters of silicon inductors fast and effectively. The IC-CAP software of Agilent used here provides an environment to build an equivalent inductor model and establish the extraction formulas/macro where the parameter extraction language (PEL) is utilized. The proposed extraction macro can extract one unique set of model parameters with satisfied accuracy for the same inductor. The systematic extraction procedures, unlike the fine-tuning of curve fitting methods, can extract the model parameters with more physically oriented meanings and judge the characteristics of inductors more effectively.

3. Extraction algorithms of the programmed extraction macro

Spiral inductors with different process structures and parameters are fabricated with standard silicon process technology. Table 1 lists the different process parameters of the inductors. The top view of the fabricated spiral inductors for measurement and simulation is shown in Fig. 1. The two-port S-parameters are measured by an Agilent-8510 network analyzer and Cascade Microtech coplanar GSG probes. The parasitic effects of probe pads are de-embedded with an "open"
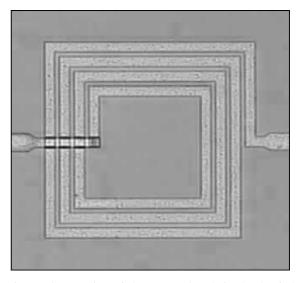

Fig. 1. The top view of the measured and simulated spiral inductors.

dummy device. While evaluating the characteristics of a one-port inductor, one terminal of the lumped equivalent model is shorted to ground. The lumped-element model of the spiral inductors used here is the same as that appeared in the literatures [6,19].

Utilizing the equivalent inductor model in Refs. [6,19], a programmed extraction macro that integrates the proposed extraction algorithms is developed to extract equivalent circuit parameters of silicon inductors fast and accurately. The extraction algorithms and the schematic processing flow of the programmed extraction macro are described below and summarized in Fig. 2. After executing the extraction macro, the measured two port S-parameters of an inductor are de-embedded with an ''open'' dummy device to remove the parasitic effects of probe pads. Then, the de-embedded S-parameters are

converted to one port Z-parameters (one port Z_{in}) by shorting another terminal to ground, and the plot of the individual real part curves of one port input impedance is displayed as shown in Fig. 3. This figure exhibits the measured real part, imaginary part and the Y_{21} curves of the sample W13 inductor as an example for demonstrating the extraction algorithms. Because R_s is nearly independent of frequency at low frequency region, R_s can be therefore extracted from the real part of one port Z_{in} at the lowest operation frequency as indicated in Fig. 3. After automatically display the plot of the imaginary part curves of one port input impedance, also as shown in Fig. 3, the one port quality factor (Q-factor) and inductance as a function of frequency are evaluated as Q-factor = Im(one port Z_{in})/ Re(one port Z_{in}) and $L =$ Im(one port Z_{in})/$(2\pi^* f)$. The parameter L_s can be ex-
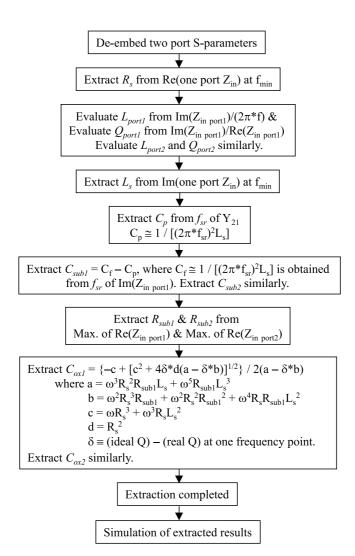

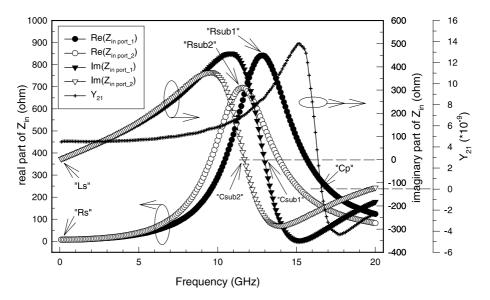Fig. 2. The schematic flow chart of the programmed extraction macro.

Fig. 3. The measured real part, imaginary part of $Z_{\text{in port1}}$ and $Z_{\text{in port2}}$ and the Y_{21} of the two port inductor for extraction (sample W13).

tracted from the imaginary part of one port Z_{in} at the lowest frequency. Observing the equivalent inductor model in Refs. [6,19] implies that the admittance of Y_{21} can be derived and expressed as $Y_{21} = [R_s + j\omega(C_pR_s^2 + C_p\omega^2L_s^2 - L_s)]/(R_s^2 + \omega^2L_s^2)$, and the self-resonance frequency of Y_{21} occurs when $(C_pR_s^2 + C_p\omega_{sr}^2L_s^2 - L_s) = 0$. Because the value of R_s is much smaller than that of $(\omega_{sr}L_s)$, the value of C_p thus can be extracted as $C_p = [L_s/(R_s^2 + \omega_{sr}^2L_s^2)] \cong (1/\omega_{sr}^2L_s)$, as indicated in Fig. 2. According to the above extraction algorithms, the equivalent model parameters of R_s, L_s and C_p are extracted.

As operation frequency increases high enough, energy transmitted into the lossy silicon substrate becomes dominant and makes C_{ox} approach electrically shorted-circuit. Therefore, the one port input impedance Z_{in} (Z_{11}) is approximately characterized by the combination of L_s, R_s, C_p, C_{sub} and R_{sub}. The parameter C_{sub} thus can be mathematically derived and extracted as: $C_{\text{sub}} = [L_s/(R_s + \omega_{sr}^2L_s^2)] - C_p = C_f - C_p$, where ω_{sr} is the self-resonance angular frequency of Z_{in}. The maximum value of real part of Z_{in} almost occurs at the same angular frequency point, ω_{sr}. Based on the above results, we could establish the transfer function near the self-resonance frequency as: $(1/R_{\text{sub}}) = (1/R_{\text{max}}) - (R_s \times C_f/L_s)$. Because the value of $(R_s \times C_f/L_s)$ is small as compared to other two terms, the value of R_{sub} can be extracted from the maximum value of real part of Z_{in}. The value of $[(R_s \times C_f \times R_{\text{sub}})/L_s] \times 100\%$ could be expressed as an optional extraction error index of R_{sub} value. The values of C_{sub} and R_{sub} are now extracted successfully according to the proposed extraction algorithms. The schematic extraction points of C_{sub} and R_{sub} are also indicated in Fig. 3.

As the inductor operates at higher frequency, the energy begins to transmit into the lossy silicon bulk. Consequently, the quality factors of silicon spiral inductors well described by $(\omega L_s/R_s)$ at low frequency are degraded rapidly due to the substrate loss effect. Therefore, the concept of deviation (δ) between the ideal and measured quality factor, as shown in Fig. 4, can be utilized to extract the value of C_{ox} according to the derived method indicated in Fig. 2. The proposed extraction algorithms for R_{sub}, C_{sub} and C_{ox} play the key techniques to program the extraction macro. Through the execution of the programmed extraction macro, all the equivalent model parameters of the silicon spiral inductors can be extracted fast and smoothly.

4. Verification of the extraction macro and discussions

After finishing the execution of the programmed macro, the measured and simulated curves, such as those shown in Figs. 5–8, are automatically displayed to verify the accuracy of the extraction. The extracted equivalent circuit parameters with different inductor structures are exhibited in Table 1. The extracted equivalent parameters in this table are directly extracted, without any additional optimization or curve fitting, by means of the extraction macro.

Comparing the extracted parameters of individual inductors in Table 1, it shows that the inductors with high substrate resistivity (W8, W24) have larger values of R_{sub}, smaller C_{ox} and higher quality factor due to its smaller substrate loss. In the mean time, the inductors with thicker metal thickness or intermetal dielectric
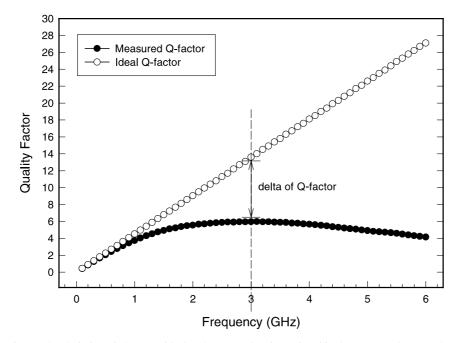
Fig. 4. The deviation (δ) between ideal and measured Q-factor is utilized to extract the C_{ox} value.
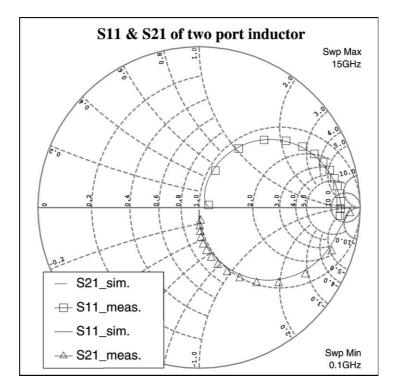

Fig. 5. The measured and simulated S_{11} and S_{21} curves of the two port inductor (sample W13).

(IMD) (W21, W24) indeed have larger Q-factor due to its smaller metal series resistance R_s and smaller sub-

strate loss. These results imply that the directly extracted equivalent model parameters implemented with the
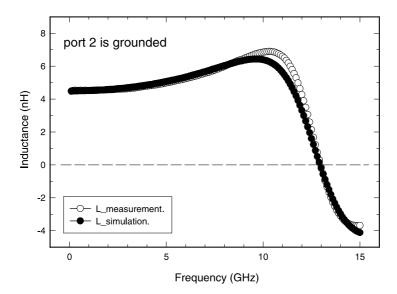
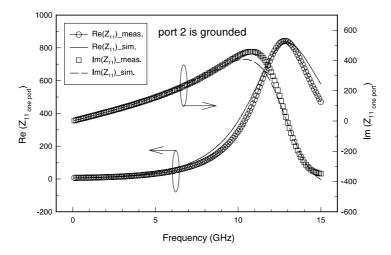Fig. 6. The measured and simulated inductance curves of the inductor with grounded port 2 (sample W13).

Fig. 7. The measured and simulated real part and imaginary part of the inductor with grounded port 2 (sample W13).

programmed extraction macro really can physically estimate and respond the characteristics of silicon spiral inductors with different structures and substrate resistivities.

Figs. 5–8 show the measured and simulated (extracted) results of sample W13 as an example for demonstrating the extraction accuracy. Table 2 lists the root mean square (RMS) extraction error of real part and imaginary part of S-parameters for the inductors listed in Table 1. Note that almost all RMS extraction errors between the measured and the simulated results are less than 5%. The discrepancy between the measured and simulated curves in Figs. 5–8 and the RMS errors are all

small enough to be accepted and well satisfy the practical requirement of the circuit simulation in the frequency range of personal wireless communication applications, such as 0.9, 1.8 or 2.4 GHz. The processing time for extracting a set of model parameters of an inductor is generally about three minutes. Such a short processing time gives a way to the extraction of high-volume inductors for building a model library of inductors.

The proposed extraction macro that based on the equivalent inductor model in Refs. [6,19] and mathematically derived extraction algorithms can extract one unique set of model parameters for the same inductor.
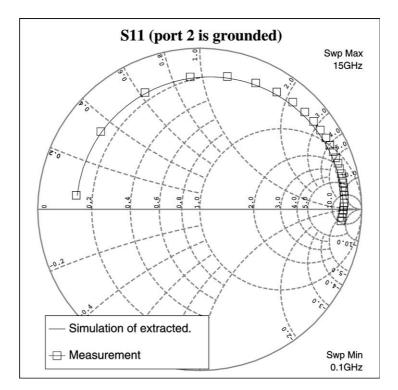
Fig. 8. The measured and simulated S_{11} curves of the one port inductor, 0.1–15 GHz (sample W13).

The unique set of model parameters overcome some drawback of EM simulation or curve fitting methods, that is, many sets of obtained inductor parameters all seem to model the behavior of the same inductor well, even though the extracted parameters are both not reasonable and physically oriented. The systematic extraction procedures, unlike the fine-tuning of curve fitting method, can extract the model parameters and judge the characteristics of inductors effectively. Through the execution of the programmed extraction macro, the dependence of the equivalent circuit parameters on different inductor structures can be reflected reasonably, as shown in Table 1.

The equivalent inductor parameters extracted by the extraction macro are for general purpose, such as the libraries of the mixed-signal devices established by the foundry companies. If the circuit designers need the model parameters utilized on specific narrow-band, slight tuning of the parameters can be easily finished to achieve the specific purpose. That is, the extracted inductor equivalent parameters can be adopted as the initial values of fine-tuning, if necessary, to obtain the user-desired inductor model parameters for RF circuit simulation. In summary, it implies that the proposed extraction macro is accurate and convenient enough to obtain the equivalent inductor circuit model parameters.

5. Conclusion

A programmed macro for extracting equivalent model parameters of silicon spiral inductors automati-

Table 2
The RMS extraction error of real part and imaginary part of S-parameters demonstrating the extraction accuracy

Device	Frequency (GHz)	Error of S_{11} (%)		Error of S_{22} (%)	
		Real	Imaginary	Real	Imaginary
W13	0.9	0.77	5.56	1.95	5.05
	1.8	1.63	2.66	0.60	2.89
	2.4	1.99	0.93	0.41	1.82
W8	0.9	3.71	6.40	4.19	6.27
	1.8	1.42	4.85	2.24	4.83
	2.4	0.16	3.98	1.07	4.01
W21	0.9	1.20	8.46	1.90	7.65
	1.8	1.53	3.40	0.17	3.32
	2.4	1.49	1.14	0.61	1.37
W24	0.9	2.01	3.04	2.40	2.88
	1.8	1.32	2.81	0.23	3.02
	2.4	3.35	2.15	1.78	2.54
W15	0.9	0.44	4.70	2.07	4.87
	1.8	2.40	2.02	0.36	2.64
	2.4	2.98	0.25	0.06	1.47

cally is presented. It can extract the equivalent model parameters of silicon spiral inductors with different structures and substrate resistivities fast and accurately. The extracted parameters also can reflect the characteristics of inductors physically and reasonably. The macro program is especially suitable for high-volume parameter extractions of many inductors to reduce the time consumption on parameter extractions effectively.

References

[1] Gray PR, Meyer RG. Future directions in silicon IC's for RF personal communications. Proc IEEE Custom Integ Circ Conf, May 1995. p. 83–90.

[2] Larson LE. Integrated circuit technology options for RFIC's present status and future directions. IEEE J Solid-State Circ 1998;33:387–99.

[3] Mikkelsen JH, Kolding TE. RF CMOS circuits target IMT-2000 applications. Microwaves & RF, July 1998. p. 99–107.

[4] Shaeffer DK, Lee TH. A 1.5-V, 1.5-GHz CMOS low noise amplifier. IEEE J Solid-State Circ 1997;32:745–59.

[5] Chang J, Abidi A, Gaitan M. Large suspended inductors on silicon and their use in a 2-m CMOS RF amplifier. IEEE Electron Dev Lett 1993;14:246–8.

[6] Nguyen NM, Meyer RG. Si IC-compatible inductors and LC passive filters. IEEE J Solid-State Circ 1990; 25:1028–31.

[7] Camilleri N, Kirchgessner J, Costa J, Ngo D, Lovelace D. Bonding pad models for silicon VLSI technologies and their effects on the noise figures of RF NPNs, IEEE Microwave and Millimeter-wave Monolithic Circ Symp Dig 1994:225–8.

[8] Burghartz JN, Soyuer M, Jenkins KA. Microwave inductors and capacitors in standard multilevel interconnect silicon technology. IEEE Trans Microwave Theory Tech 1996;44:100–4.

[9] Park M, Lee S, Kim CS, Yu HK, Koo JG, Nam KS. The detailed analysis of high Q CMOS-compatible microwave spiral inductors in silicon technology. IEEE Trans Electron Dev 1998;45:1953–9.

[10] Long JR, Copeland MA. The modeling, characterization, and design of monolithic inductors for silicon RF IC's. IEEE J Solid-State Circ 1997;32:357–69.

[11] Burghartz JN, Edelstein DC, Jenkins KA, Kwark YH. Spiral inductors and transmission lines in silicon technology using copper-damascene interconnects and low-loss substrates. IEEE Trans Microwave Theory Tech 1997; 45:1961–8.

[12] Burghartz JN, Soyuer M, Jenkins KA. Integrated RF and microwave components in BiCMOS technology. IEEE Trans Electron Dev 1996;43:1559–70.

[13] Erzgraber HB, Grabolla Th, Richter HH, Schley P, Wolff A. A novel buried oxide isolation for monolithic RF inductors on silicon. IEEE IEDM Symp Dig 1998: 535–9.

[14] Park M, Lee S, Yu HK, Koo JG, Nam KS. High Q CMOS-compatible microwave inductors using double-metal interconnection silicon technology, IEEE Microwave and Guided Wave Lett 1997;7:45–7.

[15] Yue CP, Wong SS. On-chip spiral inductors with patterned ground shields for Si-based RFIC's, IEEE VLSI Circ Symp Dig 1997:85–6.

[16] Danesh M, Long JR, Hadaway RA, Harame DL. A Q-factor enhancement technique for MMIC inductors, IEEE MTT Symp Dig 1998:183–6.

[17] Lovelace D, Camilleri N, Kannell G. Silicon MMIC inductor modeling for high volume, low cost applications. Microwave J 1994:60–71.

[18] Groves R, Stein K, Harame D, Jadus D. Temperature dependence of Q in spiral inductors fabricated in a silicon–germanium/BiCMOS technology. IEEE BCTM Dig 1996: 153–6.

[19] Ashby KB, Koullias IA, Finley WC, Bastek JJ, Moinian S. High Q inductors for wireless applications in a complementary silicon bipolar process. IEEE J Solid-State Circ 1996;31:4–8.